ITEM: **STRUCTURE, TECNAM P92 ECHO LIGHT AIRCRAFT, ZU-DMT**

1. INTRODUCTION & BACKGROUND

1.1. The wreck from a crashed Tecnam P92 Echo light aircraft, number ZU-DMT, was submitted to determine the fracture mode/s of all structural failures during operation.

1.2. Furthermore, to determine if the structural failure during operation can be attributed in any way to the rebuilding of the relevant aircraft after a previous accident (Photo 2). The aircraft completed 134 hours before the final accident.

Photo 1: Tecnam Echo P92 (courtesy Tecnam Aircraft)

Photo 2: Condition after previous accident (courtesy SACAA)

1.3. Aluminium Alloys (Courtesy ASM Handbook Volume 2)

1.3.1. Shapes. A shape is a product that is long in relation to its cross-sectional dimensions and has a cross-sectional shape other than that of sheet, plate, rod, bar, wire, or tube. Most shapes are produced by extruding or by extruding plus cold finishing; shapes are now rarely produced by rolling because of economic disadvantages. Shapes may be solid, hollow (with one or more voids), or semi-hollow. **The 6*xxx* series (Al-Mg-Si) alloys, because of their easy extrudability, are the most popular alloys for producing shapes. Some 2*xxx* and 7*xxx* series alloys are often used in applications requiring higher strength.** Standard structural shapes such as I beams, channels, and angles produced in alloy 6061 are made in different and fewer configurations than similar shapes and made of steel; the patterns especially designed for aluminum offer better section properties and greater structural stability than the steel design by using the metal more efficiently. The dimensions, weights, and properties of the alloy 6061 standard structural shapes, along with other information needed by structural engineers and designers, are contained in the Aluminum Construction Manual, published by the Aluminum Association, Inc.

1.3.2. ***Sheet.*** In the United States, sheet is classified as a flat-rolled product with a thickness of 0.006 to 0.249 in. (0.15 to 0.63 mm). Sheet edges can be sheared, slit, or sawed. Sheet is supplied in flat form, in coils, or in pieces cut to length from coils. Current facilities permit production of a limited amount of extra-large sheet, for example, up to 200 in. (5 m) wide by 1000 in. (25 m) long. The term strip, as applied to narrow sheet, is not used in the U.S. aluminum industry. Aluminum sheet usually is available in several surface finishes such as mill finish, one-side bright finish, or two-side bright finish. It may also be supplied embossed, perforated, corrugated, painted, or otherwise surface treated; in some instances, it is edge conditioned. As with aluminum plate, sheet made of the heat-treatable alloys in which copper or zinc are the major alloying constituents, notably the high-strength 2*xxx* and 7*xxx* series alloys, also is available in Alclad form for increased corrosion resistance. In addition, special composites may be obtained such as Alclad non-heat-treatable alloys for extra corrosion protection, for brazing purposes, or for special surface finishes. With a few exceptions, most alloys in the 1*xxx,* 2*xxx,* 3*xxx,* 5*xxx,* and 7*xxx* series are available in sheet form. Along with alloy 6061, they cover a wide range of applications from builders' hardware to transportation equipment and from appliances to aircraft structures.

1.3.3. **6*xxx* Series.** Alloys in the 6*xxx* series contain silicon and magnesium approximately in the proportions required for formation of magnesium silicate (Mg2Si), thus making them heat treatable. Although not as strong as most 2*xxx* and 7*xxx* alloys, 6*xxx* series alloys have good formability, weldability, machinability, and corrosion resistance, with medium strength. Alloys in this heat-treatable group may be formed in the T4 temper (solution heat treated but not precipitation heat treated) and strengthened after forming to full T6 properties by precipitation heat treatment. Uses include architectural applications, bicycle frames, transportation equipment, bridge railings, and welded structures.

1.3.4. **2*xxx* Series.** Copper is the principal alloying element in 2*xxx* series alloys, often with magnesium as a secondary addition. These alloys require solution heat treatment to obtain optimum properties; in the solution heat-treated condition, mechanical properties are similar to, and sometimes exceed, those of low-carbon steel. In some instances, precipitation heat treatment (aging) is employed to further increase mechanical properties. This treatment increases yield strength, with attendant loss in elongation; its effect on tensile strength is not as great. The alloys in the 2*xxx* series do not have as good corrosion resistance as most other aluminum alloys, and under certain conditions they may be subject to intergranular corrosion. Therefore, these alloys in the form of sheet usually are clad with a high-purity aluminum or with a magnesium-silicon alloy of the 6*xxx* series, which provides galvanic protection of the core material and thus greatly increases resistance to corrosion. Alloys in the 2*xxx* series are particularly well suited for parts and structures requiring high strength-to-weight ratios and are commonly used to make truck and aircraft wheels, truck suspension parts, aircraft fuselage and wing skins, and structural parts and those parts requiring good strength at temperatures up to 150 ℃ (300 ℉). Except for allo y 2219, these alloys have limited weldability, but some alloys in this series have superior machinability.

1.4. This report divided into the following sections:

2. APPLICABLE DOCUMENTS

(a) Tecnam P92 Echo Line Maintenance Manual.

3. DEFINITIONS

(a)	OEM	Original Equipment Manufacturer
(b)	CAA	Civil Aviation Authority
(c)	SEM	Scanning Electron Microscope
(d)	EDS	X-ray Energy Dispersive Analytical System

4. PERSONNEL

(a) The investigative member and compiler of this report is Mr C.J.C. Snyman, ID number 6406105057080. Mr Snyman is a qualified Physical Metallurgist (H.N.Dip Metallurgical Engineering, Tech. PTA), Radiation Protection Officer (RPO) registered with the National Nuclear Regulator (NNR) and Aircraft Accident Investigator (SCSI).

5. APPARATUS AND METHODOLOGY

(a) The apparatus employed for this investigation are Stereo- and Scanning Electron Microscopes and Digital Camera.
(b) The methodology included a visual investigation of supplied parts and teardown followed by a microscopic investigation.

6. INVESTIGATION

6.1. Visual, Stereo- and SE microscope Investigation.

6.1.1. <u>Horizontal/Rudder Assembly, Failure Point A.</u> The visual investigation revealed impact damages on both the rudder (Photo 3) and horizontal stabilizer (Photo 4). The fracture at the position indicated (Photo 4 and 6, blue arrows) showed typical bending fracture geometry in a downward and aft direction with no clear signs of pre-impact development. The horizontal stabilizers revealed signs of buckling most probably associated with aerodynamic forces most probably induced during flight rather than impact. Impact forces induced by the separated right hand main wing or parts thereof may have been the primary causational factor for the rudder/horizontal stabilizer in flight separation from the main fuselage.

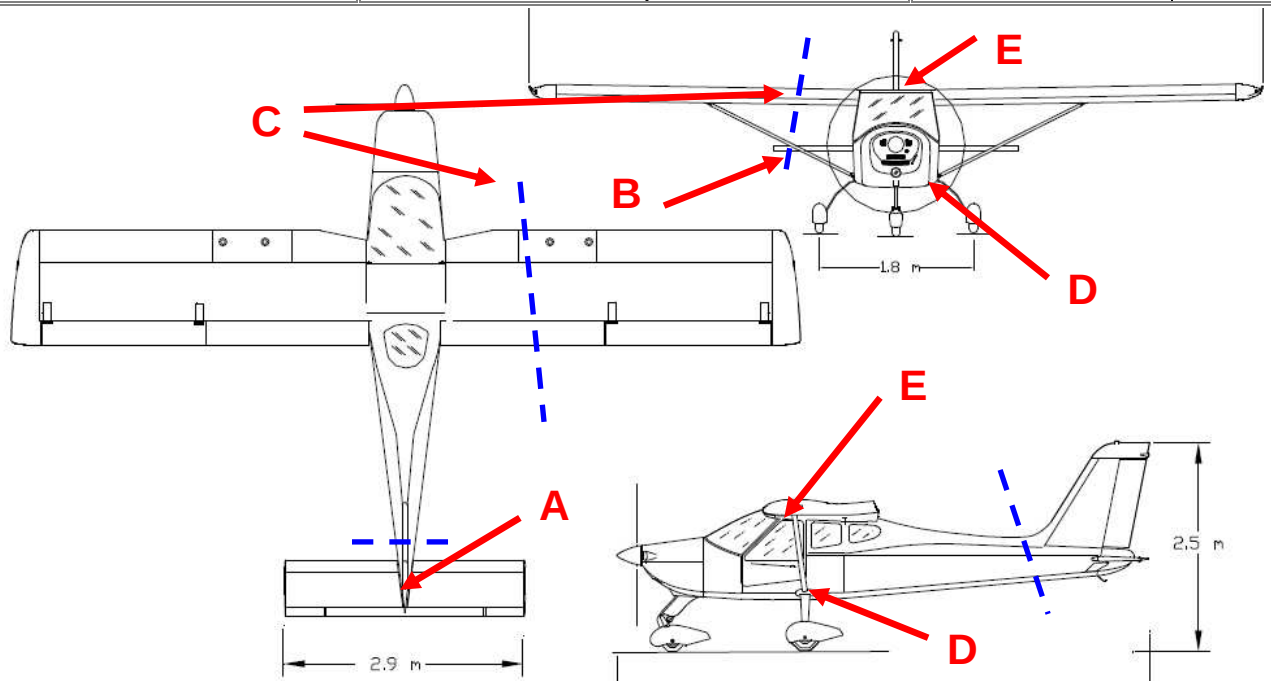

Diagram 1: General views (courtesy Tecnam)

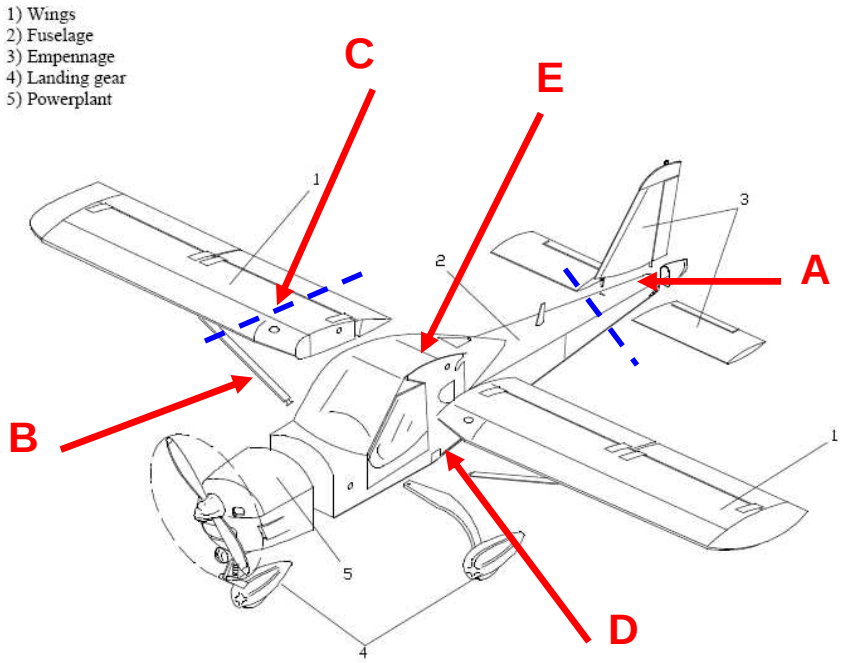

Diagram 2: Basic layout (courtesy Tecnam)

Photo 3: Rudder failure at point A (digital)

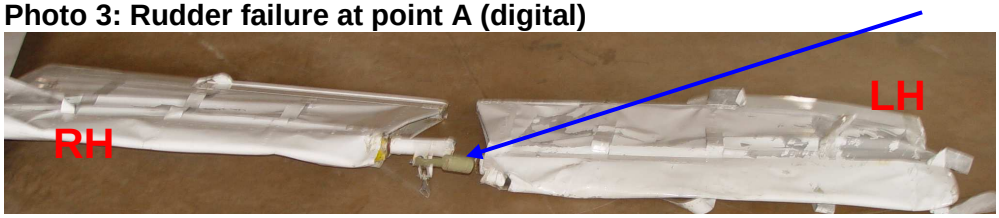

Photo 4: Horizontal stabilizer failure at point A (digital)

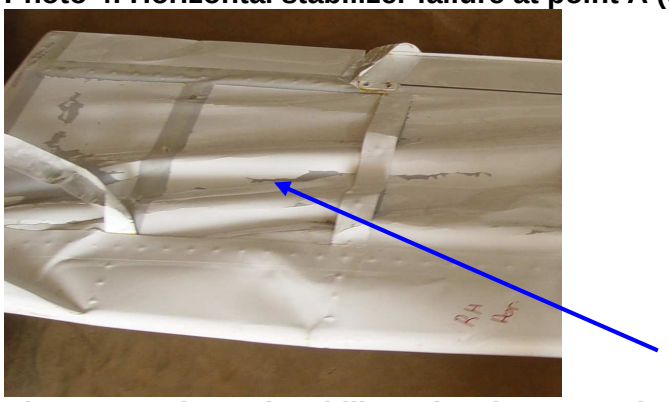

Photo 5: Horizontal stabilizer showing extensive buckling, blue arrow (digital)

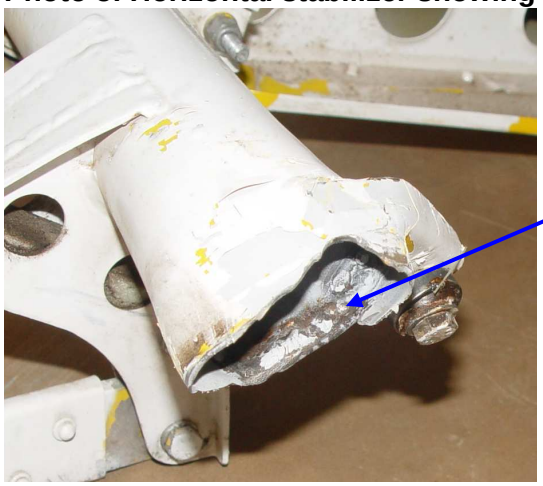

Photo 6: Horizontal stabilizer point of fracture (digital)

6.1.2. **Main Wing Assembly Failure at Points B, C and D.** The visual inspection revealed that the right hand (pilot view) wing strut fractured at point B. The fracture geometry corresponds with a bending type failure (Photo 8) and not an overload. No clear signs of pre-impact fracture development could be detected. The black rubber mark (Photo 7, blue arrow) was inflicted during contact with the right hand main landing wheel, most probably after wing separation and on impact as little bending damages were detected at the position of contact. The bending damage to the right-hand wing strut wing attachment point (Photo 9, blue arrow) corresponds to an upward and aft direction of separation for the right hand wing (Photo 9, red arrow).

The left hand wing strut fractured at point D. The damages to the fuselage attachment at point D (Photo 11) point toward a forward direction of failure. The inner steel based tube (Photo 10, red arrow) fractured at the rivet points. The fracture surface showed no clear signs of pre-impact development and the geometry corresponded with that of a ductile material under overload conditions (Photo's 12 and 13).

The visual investigation showed that the right hand wing (pilot view) separated from the remainder between the cabin truss attachment and the right hand strut attachment points at point C (Photo 14, blue dashed line). The direction of separation proved to upward and aft (Photo 14, red arrow). Taking into account the corresponding damages to the right hand flap (Photo 14, green arrow) it can be assumed that it was in position at the moment of wing separation. The wing structure revealed signs of buckling (Photo 15, red arrow) in the area between the strut and fuselage attachment points. The leading edge top and bottom L-shaped, aluminium based structural beams from the right hand wing (Photo 16, red arrows) were exposed to a SEM investigation. The fractographs (Photo's 17, 18 and 19) revealed a typical ductile material failing under overload conditions. No clear signs of pre-impact fracture development could be detected.

Photo 7: Right hand wing strut at point B (digital)

Photo 8: Right hand wing strut fracture surface (digital)

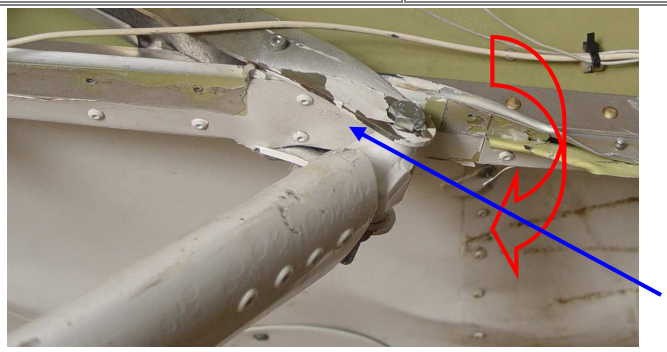

Photo 9: Right hand wing strut wing attachment point (digital)

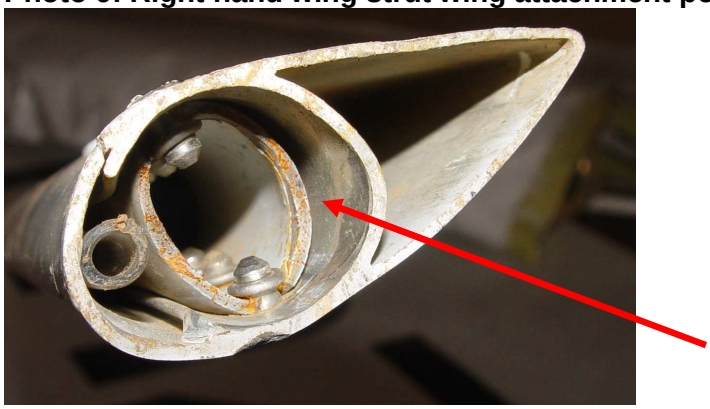

Photo 10: Left hand wing strut fracture at point D (digital)

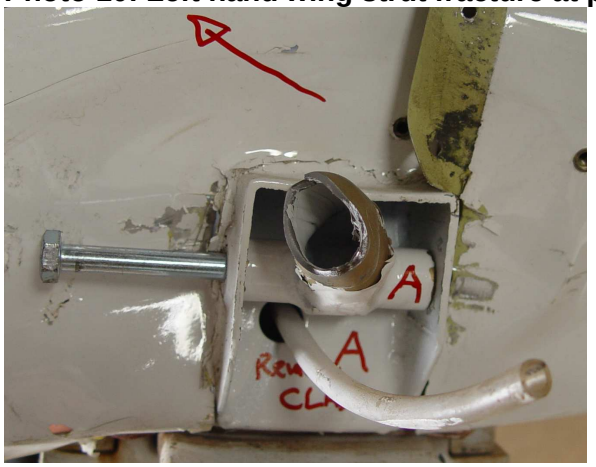

Photo 11: Left hand strut fuselage attachment at point D (digital)

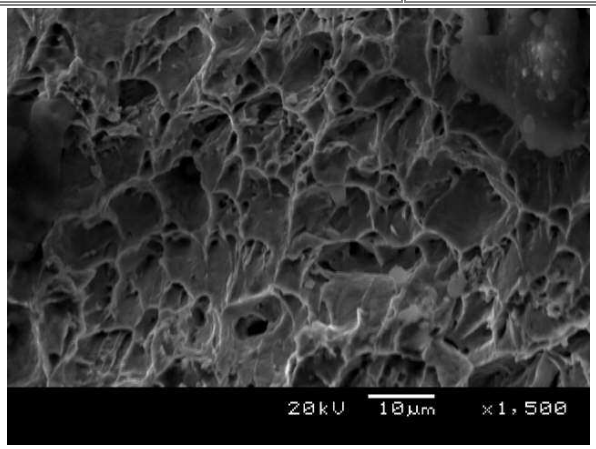

Photo 12: Fractograph, left hand strut fracture surface at point D (x1500, SEM)

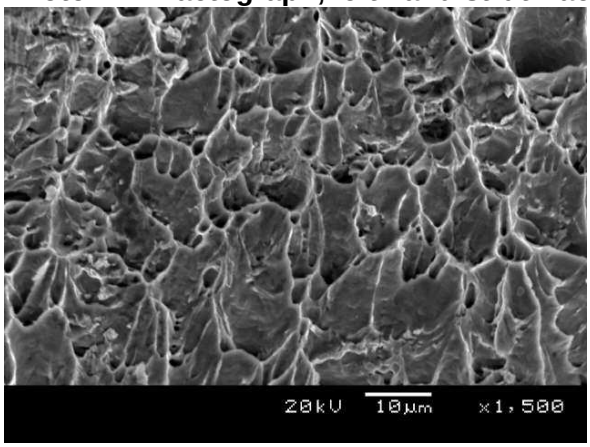

Photo 13: Fractograph, left hand strut fracture surface at point D (x1500, SEM)

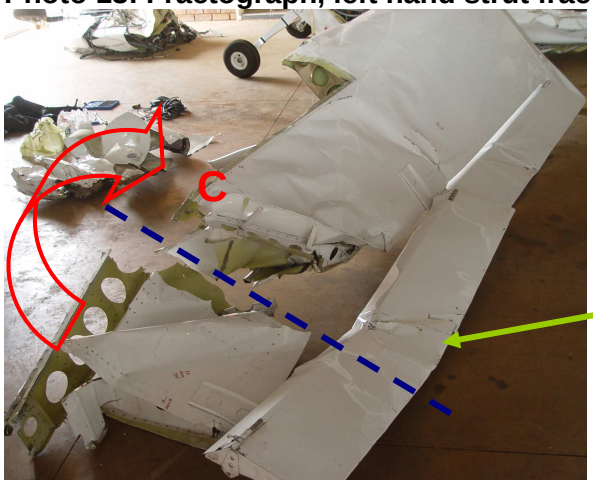

Photo 14: Right hand wing separation at point C (digital)

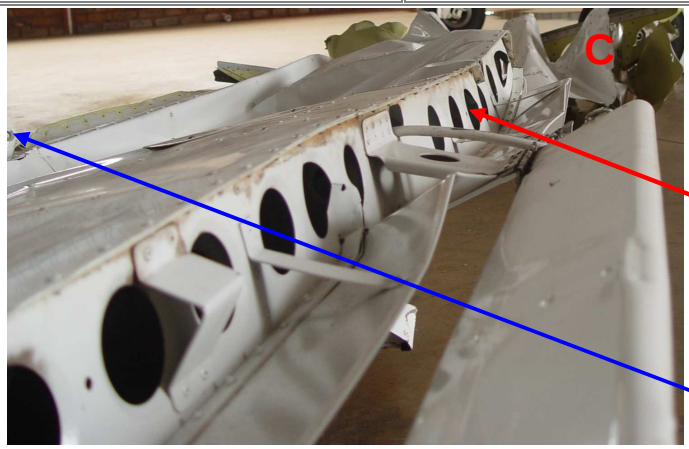

Photo 15: Right hand wing buckling damages (digital)

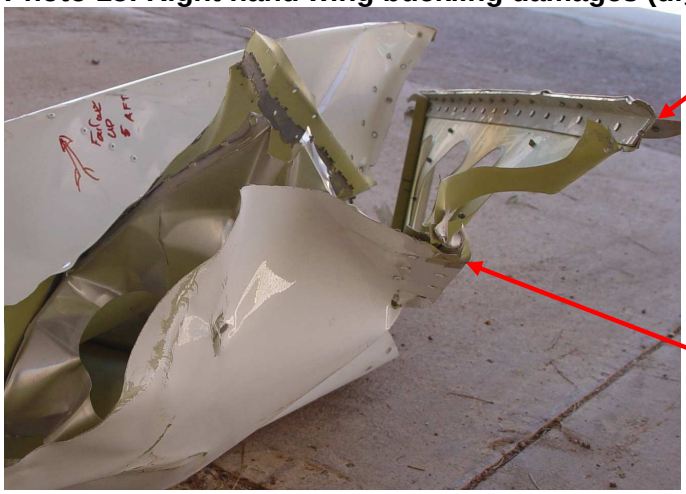

Photo 16: Right hand wing fractures at point C (digital)

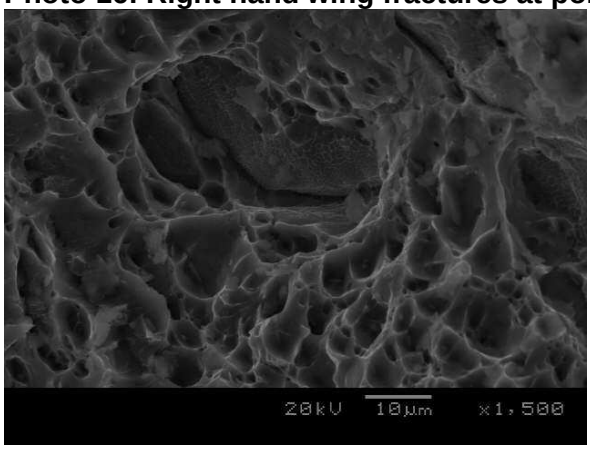

Photo 17: Fractograph, right hand wing top L-beam (x1500, SEM)

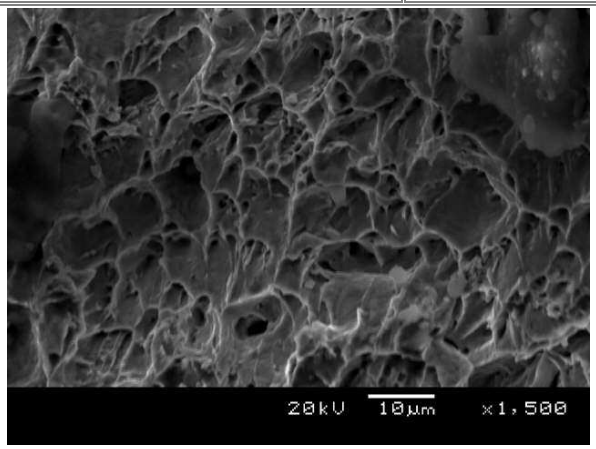

Photo 18: Fractograph, right hand wing top L-beam (x1500, SEM)

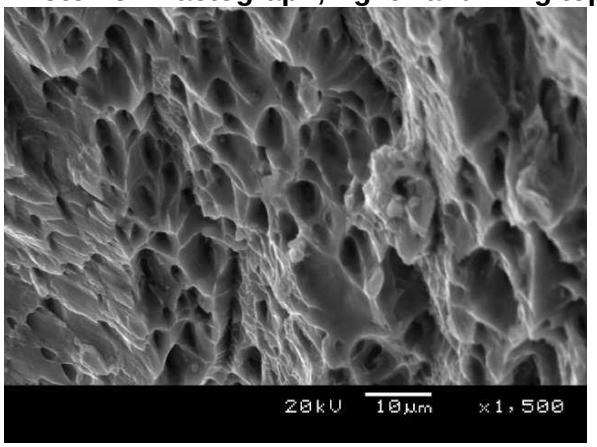

Photo 19: Fractograph, right hand wing bottom L-beam (x1500, SEM)

6.1.3. **Cabin Truss Failure at Point E.** The visual investigation revealed that the remainder of the left hand wing and centre section separated from the cabin truss at 4 primary points, E1 to E4 (Diagram 3 and Photo 20). The fracture surfaces at all four primary failure positions (Photo's 21, 22, 23 and 24) corresponds with an overload type of geometry and revealed no clear signs of pre-impact or wing separation development.

The stereomicroscope investigation confirmed some corrosion damages (Photo 25) to most of the fracture surfaces as received. These damages were most probably inflicted after impact. The non-corrosion damaged surfaces conform to overload type geometries (Photo's 26 and 27) with no clear signs of pre-impact crack formation and/or weakening of the cabin truss structure.

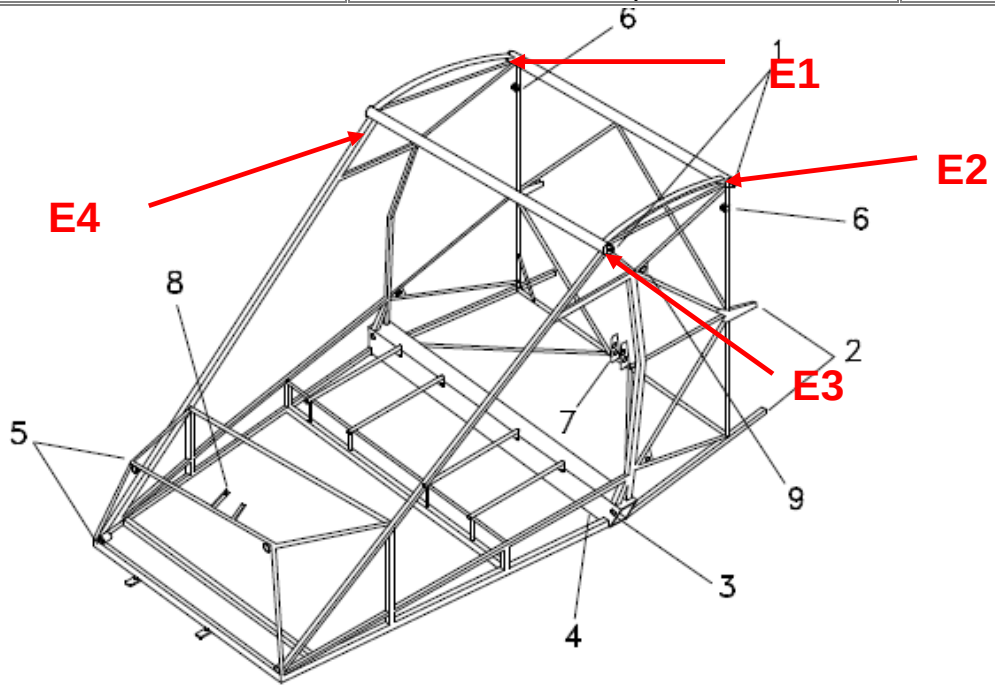

Diagram 3: Cabin truss layout with primary fractures designated by red arrows

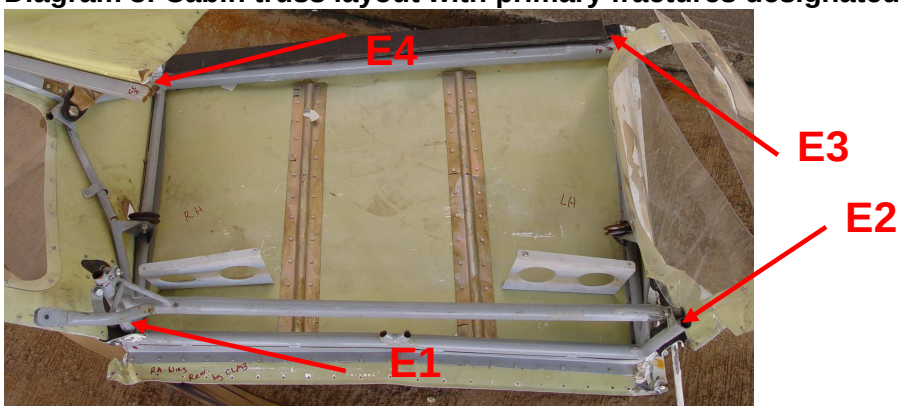

Photo 20: Primary fracture points, cabin truss (digital)

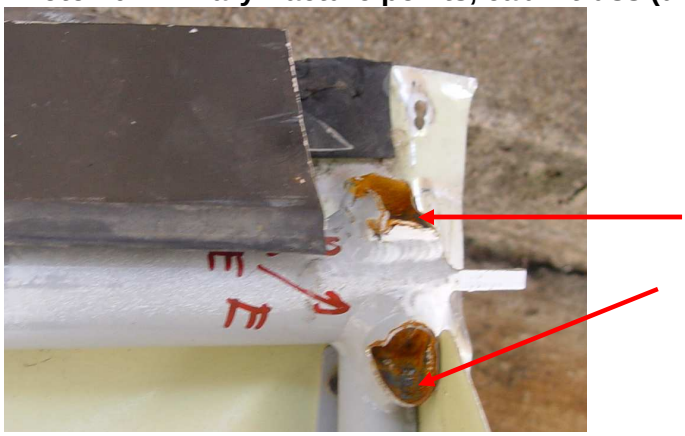

Photo 21: Fracture at point E3 (digital)

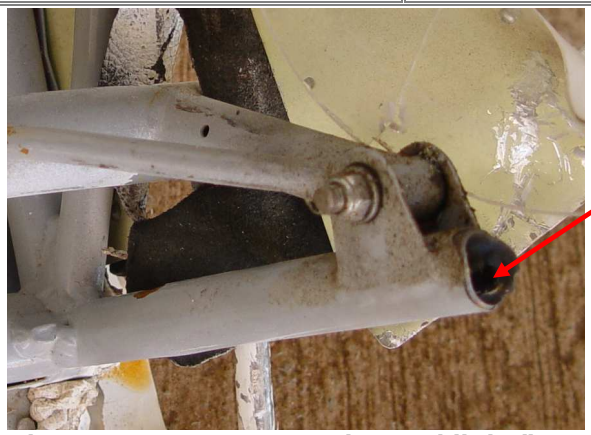

Photo 22: Fracture at point E2 (digital)

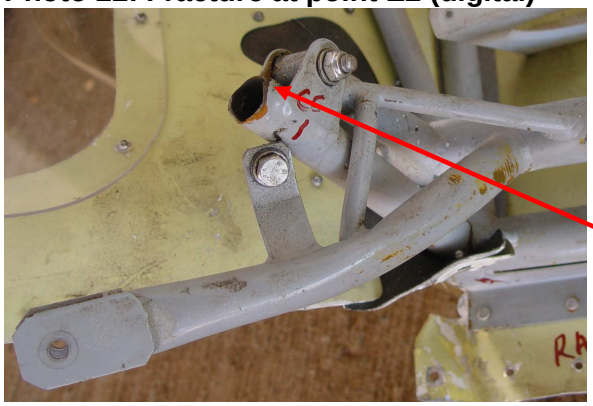

Photo 23: Fracture at point E1 (digital)

Photo 24: Fracture at point E4 (digital)

Photo 25: Fracture surface showing corrosion damages, cabin truss (stereo)

Photo 26: Fracture surface, cabin truss (stereo)

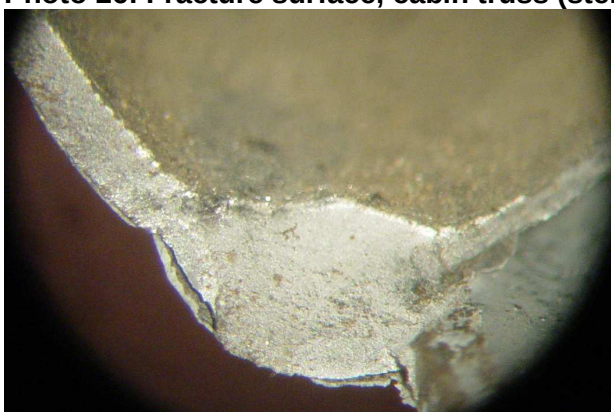

Photo 27: Fracture surface, cabin truss (stereo)

6.2. Material Analysis Results

Hardness tests**,** Spectroscopy and X-ray (EDS) analysis methods (results attached) were utilized to compare the compositions and conditions of the primary wing structural ribs and cabs A, B and C (Photo 28) to the OEM specifications.

Wing Ribs A and C compared favourable to the OEM specified **6061-T6** aluminium as well as the Spar Cab B to the specified **2024-T3** Aluminium.

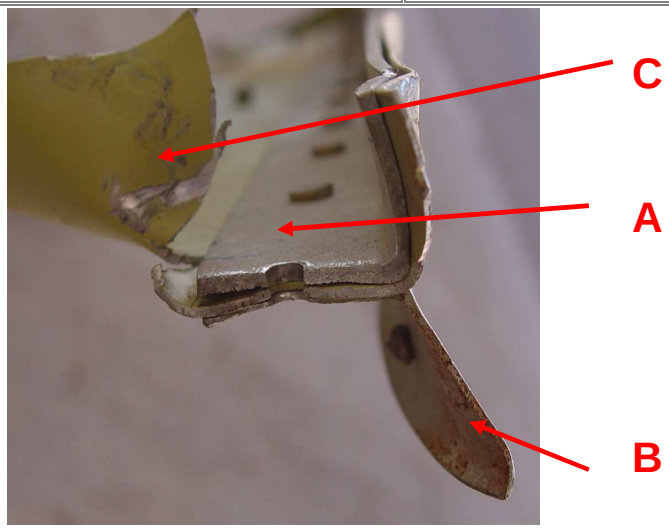

Photo 28: primary structural components, main wings

7. DISCUSSION AND CONCLUSIONS

Note: All deductions and conclusions are based on the investigation results obtained from the supplied parts only.

7.1. The rebuilding process of the relevant aircraft proved to have no effect on this accident.

7.2. All primary main wing structural member material compositions and conditions compared favourably to OEM specifications.

7.3. Under high load conditions induced by excessive **lift forces** (See diagram 4, black arrows), the wing strut will be subjected to a **tensile force** (green arrow). Two **bending moments** will be created around the strut to wing and the wing to fuselage attachment points (blue arrows). These bending moments will have a resultant **compression force** (red arrow) induced in the area between the two attachment points. This **compression force**, combined with the **bending moment** forces, will induce a **downward force** (red/grey arrow) in this section. Under excessive lift conditions, these resultant forces may induce **buckling** in the area between the strut and fuselage attachment points.

Evidence corresponding with the type of resultant forces induced on the separated right hand wing was clearly visible. The consequential buckling of the right hand wing would have been severely detrimental to the overall strength thereof. Taking into account that none of the fracture surfaces revealed any clear signs of pre-impact discrepancies, it can be derived that the right hand wing separated under high load conditions induced by excessive lift forces during operation.

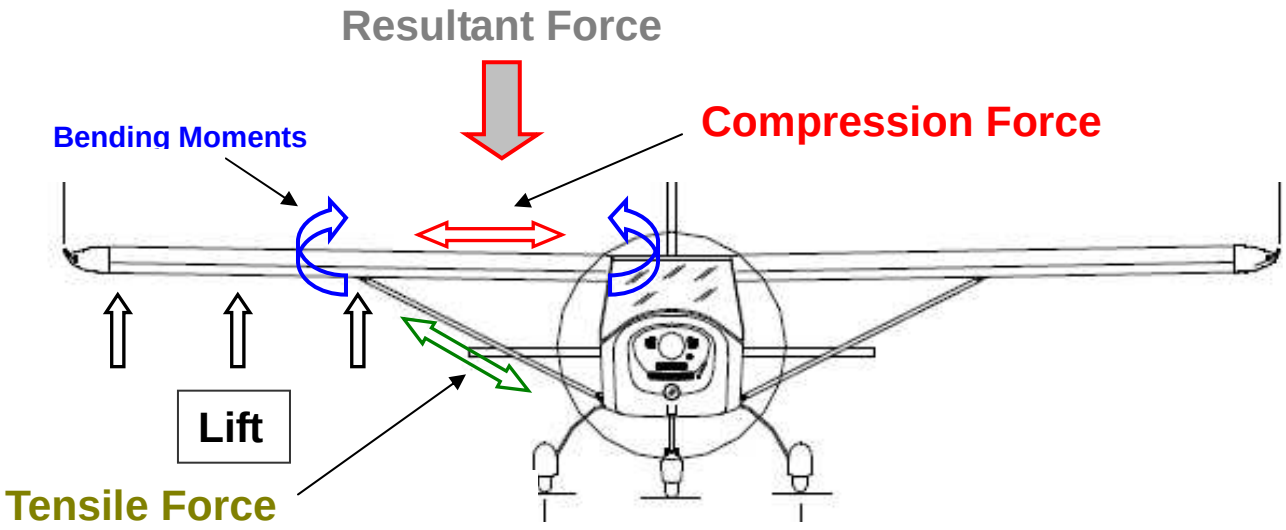

Diagram 4: Wing forces induced under high lift conditions

8. RECOMMENDATIONS

8.1. The operating envelope limitations set by the OEM and other authorities should be adhered to at all times.

9. DECLARATION

9.1. All digital images has been acquired by the author and displayed in an un-tampered manner.